Brønsted acid sites based on penta-coordinated aluminum species

Zichun Wang[1], Yijiao Jiang[2], Olivier Lafon[3], Julien Trébosc[3], Kyung Duk Kim[1], Catherine Stampfl[4], Alfons Baiker[5], Jean-Paul Amoureux[3] & Jun Huang[1]

Zeolites and amorphous silica-alumina (ASA), which both provide Brønsted acid sites (BASs), are the most extensively used solid acid catalysts in the chemical industry. It is widely believed that BASs consist only of tetra-coordinated aluminum sites (Al^{IV}) with bridging OH groups in zeolites or nearby silanols on ASA surfaces. Here we report the direct observation in ASA of a new type of BAS based on penta-coordinated aluminum species (Al^{V}) by ^{27}Al-{^{1}H} dipolar-mediated correlation two-dimensional NMR experiments at high magnetic field under magic-angle spinning. Both BAS-Al^{IV} and -Al^{V} show a similar acidity to protonate probe molecular ammonia. The quantitative evaluation of ^{1}H and ^{27}Al sites demonstrates that BAS-Al^{V} co-exists with BAS-Al^{IV} rather than replaces it, which opens new avenues for strongly enhancing the acidity of these popular solid acids.

[1] Laboratory for Catalysis Engineering, School of Chemical and Biomolecular Engineering, Sydney University, Chemical Engineering Building J01, Sydney, New South Wales 2006, Australia. [2] Department of Engineering, Macquarie University, Sydney, New South Wales 2109, Australia. [3] Univ. Lille, CNRS, UMR 8181-UCCS, Unité de Catalyse et de Chimie du Solide, F-59000 Lille, France. [4] School of Physics, Sydney University, Sydney, New South Wales 2006, Australia. [5] Institute for Chemical and Bioengineering, Department of Chemistry and Applied Bioscience, ETH Zürich, Hönggerberg, HCI, CH-8093 Zürich, Switzerland. Correspondence and requests for materials should be addressed to J.H. (email: jun.huang@sydney.edu.au) or to J.-P.A. (email: jean-paul.amoureux@univ-lille1.fr).

The need for efficient and environmentally benign chemical processes has forced the replacement of harmful and corrosive liquid acids by solid acids in various fields of catalysis, including fine chemistry[1–3], renewable energy production[4–6], oil refining and petrochemical industries[7,8]. Silicon- and aluminum-based mixed oxides provide moderate and strong Brønsted acidity and are among the most popular solid acids used in current chemical processes[7,9]. Briefly, the solid acid catalysts can protonate hydrocarbon molecules to form carbocations and drive important reactions, such as cracking, hydrocracking, isomerization, alkylation and aromatization[10–14], through surface complexes or transition states[15].

Crystalline zeolites and amorphous silica-alumina (ASA) are two main types of solid acids that contain Brønsted acid sites (BASs). It has been widely believed that only tetra-coordinated aluminum (Al^{IV}) atoms are able to contribute to the formation of BASs in nature[16]. In crystalline zeolites, the BASs are formed by protons, which compensate the negatively charged oxygens induced by the substitution of Si atoms by Al^{IV} in the framework. The structure of these sites is well known as the bridging Si(OH)Al^{IV} model (Fig. 1a)[15–17]. Replacing Si atoms by more Al^{IV} species can enhance the density of BASs, but it reduces the mean electronegativity of the framework, which thus leads to a decrease of the overall acid strength of BASs[18,19]. Similarly, Al^{IV} species incorporated into the amorphous silica network are able to generate BASs on ASA[9,20,21]. The proximity between Al^{IV} and silanol sites in ASA has recently been observed by nuclear magnetic resonance (NMR) correlation experiments between ^{29}Si and ^{27}Al nuclei, the sensitivity of which was enhanced by dynamic nuclear polarization[22]. However, the strength of these BASs is generally lower than that on crystalline zeolites[7] and thus the presence of bridging OH groups (Fig. 1a) in ASA is still strongly under debate[22,23].

A flexible coordination between the Al^{IV} atom and the neighbouring silanol oxygen atom (Fig. 1b)[9,21,24,25] or a pseudo-bridging silanol (PBS) with a nearby Al atom (Fig. 1c)[26,27] have been proposed[22], to account for the longer Al-O distances (2.94–4.43 Å) in ASA[26], with respect to those in the crystalline zeolite framework (1.88–2.0 Å)[28]. So far, most efforts focus on tuning the concentration of Al^{IV} as the main route to increase the Brønsted acidity on zeolites or silica-alumina[29–33]. However, Al^{IV} species tend to condense, to form an alumina phase at high Al/Si ratios[34–36], leading to the decrease of Brønsted acidity. For ASA containing solely BASs based on Al^{IV} species (BAS-Al^{IV}), the maximum Brønsted acidity has been obtained at 30 wt% Al loading[37,38]. In spite of the different BAS models, only Al^{IV} species have been experimentally confirmed to contribute to the formation of BASs in these catalysts. Al^{V} and Al^{VI} species have been shown to act as Lewis acid sites on ASA and zeolites, but, to the best of our knowledge, no experimental evidence of BASs involving these sites has been reported so far[39–42].
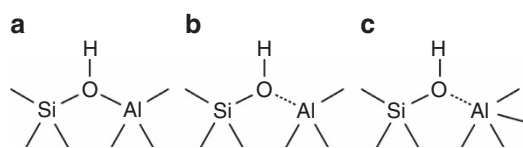
Herein, we provide the direct experimental evidence for a new type of BAS-Al^{V} in ASA by dipolar-mediated heteronuclear multiple quantum correlation (D-HMQC) two-dimensional (2D) NMR experiments, which allow the detection of protons via ^{27}Al nuclei, hereafter noted ^{27}Al-{^{1}H}, hence probing the spatial proximities between different Al species and surface protons[43–45]. These experiments show that ASA can contain a large amount of Al^{V} species located near SiOH groups. The acidity of these surface BAS-Al^{V} sites has been demonstrated in this research by the adsorption of basic ammonia molecules, which react with BAS-Al^{V} to form surface ammonium ions.

Results

Probing the connectivity between Al^{V} species and SiOH groups. The ASAs used in this work (see Supplementary Methods) have been prepared according to a previously described procedure[9], which generates ASA nanoparticles with a large amount of Al^{V} species. The ASA powders are designated as SA/X, where X is 10 or 50, indicating the molar fraction of Al in the precursor with respect to the total amount of Al and Si atoms. The obtained ASAs have tunable BAS acidity strengths ranging from moderate (SA/10 has an acidity close to zeolite H-X) to large (SA/30–70 have stronger BASs than zeolites H-Y and ZSM-5), depending on the aluminum content, as confirmed by both ^{13}C magic angle spinning (MAS) NMR investigation with probe molecule acetone and ammonia-temperature program desorption (TPD)[9]. The ASAs exhibited excellent catalytic performances for the conversion of phenylglyoxal with various alcohols, better than that of dealuminated zeolite Y, which hitherto was considered to be the most active solid acid in phenylglyoxal conversion[2].

The formation of BAS requires the aluminum atoms to be close to SiOH groups. Such proximity induces a dipolar coupling between ^{27}Al and ^{1}H nuclei, which can efficiently be probed by D-HMQC NMR 2D experiments based on coherence transfers via the ^{1}H-^{27}Al dipolar couplings[46,47]. As shown in Fig. 2, the correlation at $\delta_{27A} = 50$ p.p.m. and $\delta_{1H} = 1.9$ p.p.m. in the ^{27}Al-{^{1}H} D-HMQC 2D spectrum of dehydrated SA/50 indicates a close proximity between Al^{IV} species and the proton of SiOH groups. This correlation is ascribed to the Si-OH···Al^{IV} coordination: the typical BAS-Al^{IV} often described for ASA (Fig. 1c)[16]. A very weak correlation at $\delta_{27Al} = 10$ p.p.m. and $\delta_{1H} = 1.1$ p.p.m. is assigned to the non-acidic terminal Al^{VI}OH groups often observed on the surface of silica-alumina or zeolites, whereas the low-field broad hump at ca. 6 p.p.m. in the
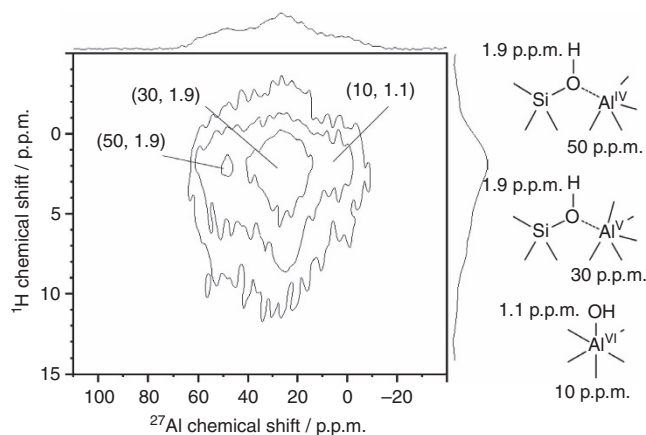
Figure 1 | Proposed models for BASs in silica-alumina catalysts. (a) BAS consisting of a bridging silanol site bonded to Al^{IV} site (Si(OH)Al) in zeolites[15]. **(b)** BAS consisting of the flexible coordination between silanol oxygen and neighbouring Al^{IV} (ref. 24). **(c)** BAS consisting of PBS interacting with Al^{IV} site[27]. In that later case, the dotted line does not denote a covalent bond but only the close proximity between O and Al atoms.

Figure 2 | ^{27}Al-{^{1}H} D-HMQC 2D spectrum of SA/50. The sample was dehydrated at 723 K for 12 h under vacuum and recorded at 18.8 T with a MAS frequency of $\nu_R = 20$ kHz and $\tau_{rec} = 1.0$ ms. The spectrum reveals that the proximity between SiOH groups and Al^{V} species is dominant.

[1]H dimension could be caused by the small fraction of hydrogen-bonded AlOH groups[16]. Nevertheless, the most intense correlation is observed between Al[V] species ($\delta_{27A} = 30$ p.p.m.) and SiOH protons ($\delta_{1H} = 1.9$ p.p.m.), which indicates the close proximity between SiOH groups and Al[V] species, and the presence of Si-OH$\cdots$Al[V] coordination (Fig. 2) in dehydrated SA/50.

Al[V]-based BASs. In zeolites, the substitution of a framework Si atom by an Al[IV] one to form one SiOHAl acid site (Fig. 1a) can shift the ^{1}H NMR signal of SiOH from ca. 1.8 to 3.6–5.2 p.p.m. (ref. 16). For these catalysts, BAS could be directly evidenced by the cross-peak in ^{27}Al-{[1]H} D-HMQC 2D spectrum between Al[IV] species ($\delta_{27Al} = 60$ p.p.m.) and the bridging OH groups ($\delta_{1H} = 4.3$ p.p.m.)[43]. However, previous works have shown that the Al atoms with neighbouring SiOH groups (Fig. 1b,c) do not produce such a shift of the ^{1}H MAS signal of these groups[5,6,9,16,20,21]. Supplementary Fig. 1a,b show that the ^{1}H signal of SA/10 and SA/50 is centred around 1.9 p.p.m., thus indicating a majority of flexible or PBS coordination rather than zeolitic bridging coordination between SiOH groups and either Al[IV] or Al[V] species.

Experiments using probe molecules have confirmed the role of flexible or PBS Si-OH$\cdots$Al[IV] coordination as BAS in ASA[5,6,9,16,20,21]. Similar methods using ammonia probe molecules were applied here to demonstrate the acidity of the Si-OH$\cdots$Al[V] coordination observed in dehydrated SA/10 and SA/50 (ref. 16). For these samples loaded with ammonia, the ^{1}H signal of ammonium ions was observed at $\delta_{1H} = 6.7$ p.p.m., as shown in Supplementary Fig. 1c,d, and commented in Supplementary Note 1. The formation of these ions shows that ammonia reacts with BAS of SA/10 and SA/50.

^{27}Al-{[1]H} D-HMQC experiments were also carried out to determine the nature of BAS, which protonate the ammonia molecules. Such a strategy based on [1]H-^{27}Al correlations has been applied for [Al]MCM-41 loaded with ammonia. For such catalysts, ammonium ions ($\delta_{1H} = 6.7$ p.p.m.) were only coupled to Al[IV] species ($\delta_{27A} = 56$ p.p.m.)[44]. Hence, there was only evidence for BAS-Al[IV] on the surface of [Al]MCM-41, which protonated ammonia to ammonium ions. As seen in Fig. 3, a correlation between NH$_4^+$ ions ($\delta_{1H} = 6.7$ p.p.m.) and Al[IV] ($\delta_{27Al} = 50$ p.p.m.) is also observed in ^{27}Al-{[1]H} D-HMQC spectra of SA/10 and SA/50, showing that the BAS-Al[IV] sites are also present on the surface of ASAs (Fig. 4a). Interestingly, these spectra also exhibit cross-peaks between Al[V] species ($\delta_{27Al} = 30$ p.p.m.) and NH$_4^+$ ions ($\delta_{1H} = 6.7$ p.p.m.) in both SA/10 and SA/50. As seen in Fig. 3e, the intensity of this Al[V]-NH$_4^+$ cross-peak is comparable to that of the Al[IV]-NH$_4^+$ one. Given the BAS density ranging from 0.16 to 0.36 H$^+$ nm^{-2} in the investigated ASA samples (Supplementary Table 1), each ammonia molecule only interacts with one BAS. The distance between the aluminium atom and the neighbouring silanol oxygen in ASA ranges from ca. 2.94 to 4.43 Å[26] and the N–H bond length in ammonia is only 1.02 Å[48]. As the heteronuclear coherence transfer in ^{27}Al-{[1]H} D-HMQC is only effective up to a few angstroms, the protons of Si-O$^-$(NH$_4$)$^+\cdots$Al environment only interact with the neighbouring Al. The observation of an Al[V]-NH$_4^+$ cross-peak in Fig. 3 at (30, 6.7) p.p.m. directly confirmed that ammonia is protonated on a BAS containing Al[V]: the Si-OH$\cdots$Al[V] group.

The comparison of Supplementary Fig. 1c,d shows that more ammonia molecules are protonated on BAS-Al[V] in SA/50 than in SA/10. Combined with quantitative ^{1}H NMR investigations (Supplementary Fig. 1) and the quadrupolar parameters (Supplementary Table 2 and Supplementary Note 2) obtained
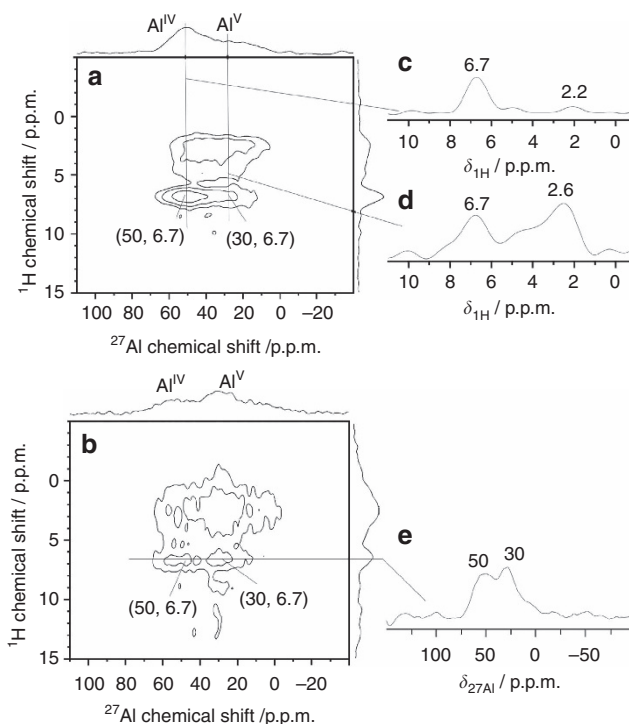

Figure 3 | ^{27}Al-{[1]H} D-HMQC 2D spectra of ammonia-loaded ASA samples. The dehydrated SA/10 (**a**) and SA/50 (**b**) samples were loaded with ammonia and evacuated at 373 K for 1h, and the spectra were recorded at 18.8 T with $\nu_R = 20$ kHz and $\tau_{rec} = 900$ μs. The ^{1}H slices at the shifts of Al[IV] and Al[V] sites of SA/10 extracted from the 2D spectrum (**a**) are displayed in subfigures (**c,d**), respectively. The subfigure (**e**) shows the ^{27}Al slice at the shift of NH$_4^+$ protons in SA/50 extracted from the spectrum (**b**).
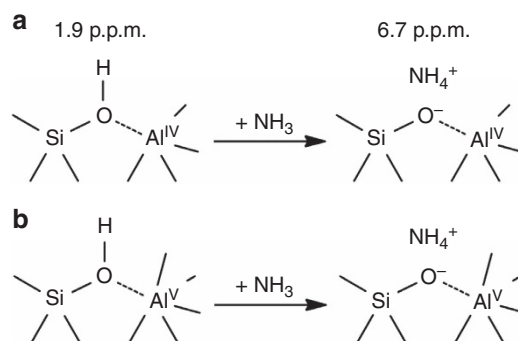

Figure 4 | Proposed proton transfer between BAS and ammonia molecules. (**a**) Ammonia protonated on conventional acidic BAS-Al[IV]. (**b**) BAS-Al[V] formed on ASA is able to transfer hydroxyl proton to ammonia, showing similar acidic properties as BAS-Al[IV].

from ^{27}Al one-dimensional MAS (Supplementary Fig. 3) and 2D multiple quantum MAS (Supplementary Fig. 2) NMR experiments, the analysis of ^{27}Al cross-peak intensities in ^{27}Al-{[1]H} D-HMQC spectra (Supplementary Fig. 4 and Supplementary Note 3) revealed that the population densities of both BAS-Al[IV] and -Al[V] on SA/50 (0.078 and 0.053 mmol g^{-1}) were both higher than those of SA/10 (0.058 and 0.039 mmol g^{-1}). This result suggests that BAS-Al[IV] and -Al[V] can co-exist on the surface rather than replacing each other and the population of both acid sites can be amplified by increasing Al content. Thus, this observation is promising for enhancing the population of BAS on ASA without limitation imposed by the Al

contents. It should be noted that the F_2 projections of ^{27}Al-$\{^1H\}$ D-HMQC 2D spectra are almost identical for dehydrated and ammonia-loaded SA/50 (see Supplementary Fig. 5 and Supplementary Note 4). Therefore, Si-OH⋯Al^V and Si-OH⋯Al^{IV} coordinations remained unchanged after the protonation of ammonia (as shown in Fig. 4). No Si-OH⋯Al^{IV} have been transferred to Si-OH-Al^V permanently after the adsorption of ammonia. In other words, the NMR results do not show the formation of permanent covalent bridges between silicate and Al^{IV} or Al^V sites in ASA samples after the deprotonation of BAS reacting with ammonia. Ammonia partially interacting with surface Al^{IV} or Al^V sites (Fig. 3b and Supplementary Fig. 6) was also observed, which has been assigned to ammonia adsorbed on Lewis sites (Supplementary Note 5).

As shown in Fig. 1, a surface bridging SiOHAl (Fig. 1a), a flexible coordination of SiOH and Al (Fig. 1b), or a pseudo-bridge between SiOH and Al atom (Fig. 1c) have been proposed for the formation of BAS-Al^{IV} on ASAs. By analogy, similar structures might also contribute to the formation of BAS-Al^V. The PBS model permits an explanation of the observation of the ^1H NMR signal of SiOH at 1.9 p.p.m. in both Fig. 2 and Supplementary Fig. 1, whereas this ^1H signal of bridging OH groups (Fig. 1a) should occur at 3.6–5.2 p.p.m. If bridging OH groups are present in the investigated ASAs, their concentration must be below the limit of detection of the one-dimensional NMR MAS spectra of Supplementary Fig. 1. Nevertheless, the current NMR data cannot rule out, in addition to PBS, the presence of bridging silanol groups in low concentration in ASA samples. These elusive strong BASs may also contribute to the catalytic activity in spite of their low concentration. The identification of all catalytic BASs in ASAs is beyond the scope of the present study, which is mainly to report the existence of BASs based on Al^V environments. A final assessment of the local structure of BAS-Al^V will require further experimental and theoretical work.

In summary, a new type of BAS-Al^V has been directly observed by ^{27}Al-$\{^1H\}$ D-HMQC NMR spectroscopy. Hitherto, it was widely accepted that Al^V sites only provide Lewis acidity[39–42], and that solely Al^{IV} ones contribute to the formation of BASs in aluminosilicate. However, we prove here by NMR experiments that similar to Al^{IV} sites, Al^V ones interact with neighbouring SiOH groups in ASA and behave as BASs in agreement with the PBS model. BAS-Al^{IV} and -Al^V seem to be structurally similar and show comparable acidity to protonate ammonia. Finally, a very important implication emerging from this work is that both Al^{IV} and Al^V species can co-exist on the surface of ASA. This feature facilitates that the total population density of BAS can be increased up to 70% by increasing the Al content, an amount much higher than the maximum Al loading of ca. 30% at which maximum acidity on ASA containing exclusively BAS-Al^{IV} is achieved[37,38]. Hence, our findings not only report the existence of a new type of BAS in nature, but also open new avenues for creating high-performance solid acid catalysts containing Al^V species, which will be promising for sustainable oil-refining and many industrial chemical processes.

Methods

^{27}Al-$\{^1H\}$ D-HMQC 2D experiment. All NMR experiments were recorded on a Bruker Avance III 18.8 T (^1H Larmor frequency of 800 MHz) spectrometer equipped with a 3.2 mm double-resonance MAS probe, in which rotors were spun at $\nu_R = 20$ kHz. In the D-HMQC sequence, we have detected the ^{27}Al nuclei to benefit from their fast longitudinal relaxation times and the ^1H-^{27}Al dipolar couplings were reintroduced by applying a SR4$_1^2$ recoupling on the ^1H channel[49]. The ^1H radiofrequency amplitudes for the 90° pulses and the SR4$_1^2$ recoupling were equal to $\nu_1 = 62.5$ and 40 kHz, respectively. The central transition selective pulse lengths on ^{27}Al were 8 and 16 μs for 90° and 180° pulses, respectively, that is, radiofrequency field amplitude $\nu_1 = 10$ kHz. The total dipolar recoupling time, τ_{rec}, ranged from 700 to 1,000 μs depending on the

sample. The 2D spectra resulted from the accumulation of 512 transients for each of 20 t_1 increments with $\Delta t_1 = 50$ μs and a recycle delay = 1 s, that is, a total experiment time of about 3 h. Additional details about NMR experiments are given in the Supplementary Methods.

References

1. Corma, A., Iborra, S. & Velty, A. Chemical routes for the transformation of biomass into chemicals. *Chem. Rev.* **107**, 2411–2502 (2007).
2. Wang, Z., Jiang, Y., Baiker, A. & Huang, J. Efficient acid-catalyzed conversion of phenylglyoxal to mandelates on flame-derived silica/alumina. *ACS Catal* **3**, 1573–1577 (2013).
3. Wang, Z., Jiang, Y., Hunger, M., Baiker, A. & Huang, J. Catalytic performance of Brønsted and Lewis acid sites in phenylglyoxal conversion on flame-derived silica-zirconia. *ChemCatChem* **6**, 2970–2975 (2014).
4. Huber, G. W., Iborra, S. & Corma, A. Synthesis of transportation fuels from biomass: chemistry, catalysts, and engineering. *Chem. Rev.* **106**, 4044–4098 (2006).
5. Huang, J., Jiang, Y., van Vegten, N., Hunger, M. & Baiker, A. Tuning the support acidity of flame-made Pd/SiO$_2$-Al$_2$O$_3$ catalysts for chemoselective hydrogenation. *J. Catal.* **281**, 352–360 (2011).
6. Wang, Z. *et al.* Palladium-doped silica–alumina catalysts obtained from double-flame FSP for chemoselective hydrogenation of the model aromatic ketone acetophenone. *J. Catal.* **302**, 10–19 (2013).
7. Corma, A. Inorganic solid acids and their use in acid-catalyzed hydrocarbon reactions. *Chem. Rev.* **95**, 559–614 (1995).
8. Busca, G. Acid catalysts in industrial hydrocarbon chemistry. *Chem. Rev.* **107**, 5366–5410 (2007).
9. Huang, J., van Vegten, N., Jiang, Y., Hunger, M. & Baiker, A. Increasing the Brønsted acidity of flame-derived silica/alumina up to zeolitic strength. *Angew. Chem. Int. Ed.* **49**, 7776–7781 (2010).
10. Engelhardt, J. & Hall, W. K. Peculiarities observed in H-D exchange between perdeuterioisobutane and H-zeolites. *J. Catal.* **151**, 1–9 (1995).
11. Hua, W. *et al.* H/D exchange reaction between isobutane and acidic USY zeolite: a mechanistic study by mass spectrometry and *in situ* NMR. *J. Catal.* **204**, 460–465 (2001).
12. Olah, G. A. Carbocations and electrophilic reactions. *Angew. Chem. Int. Ed.* **12**, 173–212 (1973).
13. Olah, G. A. *Friedel-Crafts Chemistry* (Wiley-Interscience, 1973).
14. Olah, G. A. My search for carbocations and their role in chemistry (Nobel lecture). *Angew. Chem. Int. Ed.* **34**, 1393–1405 (1995).
15. Weitkamp, J. & Hunger, M. in *Studies in Surface Science and Catalysis* (eds Ejka, J., van Bekkum, H., Corma, A. & Schüth, F.) 787–835 (Elsevier, 2007).
16. Jiang, Y., Huang, J., Dai, W. & Hunger, M. Solid-state nuclear magnetic resonance investigations of the nature, property, and activity of acid sites on solid catalysts. *Solid State Nucl. Magn. Reson.* **39**, 116–141 (2011).
17. Li, S. *et al.* Brønsted/Lewis acid synergy in dealuminated HY zeolite: a combined solid-state NMR and theoretical calculation study. *J. Am. Chem. Soc.* **129**, 11161–11171 (2007).
18. Jacobs, P. A., Mortier, W. J. & Uytterhoeven, J. B. Properties of zeolites in relation to their electronegativity - acidity, carboniogenic activity and strength of interaction in transition-metal complexes. *J. Inorg. Nucl. Chem.* **40**, 1919–1923 (1978).
19. Mortier, W. J. Zeolite electronegativity related to physicochemical properties. *J. Catal.* **55**, 138–145 (1978).
20. Wang, Z. *et al.* One-step room-temperature synthesis of Al MCM-41 materials for the catalytic conversion of phenylglyoxal to ethylmandelate. *ChemCatChem* **5**, 3889–3896 (2013).
21. Luo, Q. *et al.* Using trimethylphosphine as a probe molecule to study the acid states in Al-MCM-41 materials by solid-state NMR spectroscopy. *J. Phys. Chem. B* **107**, 2435–2442 (2003).
22. Valla, M. *et al.* Atomic description of the interface between silica and alumina in aluminosilicates through dynamic nuclear polarization surface-enhanced nmr spectroscopy and first-principles calculations. *J. Am. Chem. Soc.* **137**, 10710–10719 (2015).
23. Hensen, E. J. M. *et al.* Acidity characterization of amorphous silica-alumina. *J. Phys. Chem. C* **116**, 21416–21429 (2012).
24. Omegna, A., van Bokhoven, J. A. & Prins, R. Flexible aluminum coordination in alumino-silicates. Structure of zeolite H-USY and amorphous silica-alumina. *J. Phys. Chem. B* **107**, 8854–8860 (2003).
25. Hunger, M., Schenk, U., Breuninger, M., Glaser, R. & Weitkamp, J. Characterization of the acid sites in MCM-41-type materials by spectroscopic and catalytic techniques. *Micro. Meso. Mater.* **27**, 261–271 (1999).

26. Chizallet, C. & Raybaud, P. Pseudo-bridging silanols as versatile Brønsted acid sites of amorphous aluminosilicate surfaces. *Angew. Chem. Int. Ed.* **48,** 2891–2893 (2009).

27. Chizallet, C. & Raybaud, P. Acidity of Amorphous silica-alumina: from coordination promotion of Lewis sites to proton transfer. *ChemPhysChem* **11,** 105–108 (2010).

28. Eichler, U., Brandle, M. & Sauer, J. Predicting absolute and site specific acidities for zeolite catalysts by a combined quantum mechanics interatomic potential function approach. *J. Phys. Chem. B* **101,** 10035–10050 (1997).

29. Dewitte, B. M., Grobet, P. J. & Uytterhoeven, J. B. Pentacoordinated aluminum in noncalcined amorphous aluminosilicates, prepared in alkaline and acid-medium. *J. Phys. Chem.* **99,** 6961–6965 (1995).

30. Williams, M. F. et al. Hydrogenation of tetralin on silica-alumina-supported Pt catalysts I. Physicochemical characterization of the catalytic materials. *J. Catal.* **251,** 485–496 (2007).

31. de Boer, J. H. Constitution and properties of silica-alumina-catalysts. *Discuss. Farad. Soc.* **52,** 109–112 (1971).

32. Haag, W. O., Lago, R. M. & Weisz, P. B. The active site of acidic aluminosilicate catalysts. *Nature* **309,** 589–591 (1984).

33. Xu, B. et al. Strong Brønsted acidity in amorphous silica − aluminas. *J. Phys. Chem. C* **111,** 12075–12079 (2007).

34. Matsumoto, A., Chen, H., Tsutsumi, K., Grun, M. & Unger, K. Novel route in the synthesis of MCM-41 containing framework aluminum and its characterization. *Micro. Meso. Mater.* **32,** 55–62 (1999).

35. Eimer, G. A., Pierella, L. B., Monti, G. A. & Anunziata, O. A. Synthesis and characterization of Al-MCM-41 and Al-MCM-48 mesoporous materials. *Catal. Lett.* **78,** 65–75 (2002).

36. Hensen, E. et al. Formation of acid sites in amorphous silica-alumina. *J. Catal.* **269,** 201–218 (2010).

37. Tanabe, K. *Solid Acids and Bases and Their Catalytic Properties* (Academic Press, 1970).

38. Hunger, M. et al. High-resolution proton magnetic-resonance and catalytic studies concerning Brønsted centers of amorphous Al₂O₃-SiO₂ solids. *Chem. Phys. Lett.* **100,** 29–33 (1983).

39. Coster, D., Blumenfeld, A. L. & Fripiat, J. J. Lewis acid sites and surface aluminum in aluminas and zeolites: a high-resolution NMR study. *J. Phys. Chem.* **98,** 6201–6211 (1994).

40. Ma, D. et al. An investigation of the roles of surface aluminum and acid sites in the zeolite MCM-22. *Chem. Eur. J.* **8,** 162–170 (2002).

41. Borade, R., Adnot, A. & Kaliaguine, S. An XPS study of acid sites in dehydroxylated Y zeolites. *J. Mol. Catal.* **61,** L7–L14 (1990).

42. Kwak, J. H., Mei, D., Peden, C. H. F., Rousseau, R. & Szanyi, J. (100) facets of gamma-Al₂O₃: the active surfaces for alcohol dehydration reactions. *Catal. Lett.* **141,** 649–655 (2011).

43. Li, S. et al. Extra-framework aluminium species in hydrated faujasite zeolite as investigated by two-dimensional solid-state NMR spectroscopy and theoretical calculations. *Phys. Chem. Chem. Phys.* **12,** 3895–3903 (2010).

44. Janicke, M. T. et al. Aluminum incorporation and interfacial structures in MCM-41 mesoporous molecular sieves. *J. Am. Chem. Soc.* **120,** 6940–6951 (1998).

45. Wang, Y. Y., Mu, Y., Sun, Y. J. & Li, J. Y. Two new four-connected zeolite-like magnesium aluminophosphates with intersecting 8-ring channels. *RSC Adv.* **4,** 56288–56293 (2014).

46. Lafon, O. et al. Indirect detection via spin-1/2 nuclei in solid state NMR spectroscopy: application to the observation of proximities between protons and quadrupolar nuclei. *J. Phys. Chem. A.* **113,** 12864–12878 (2009).

47. Tricot, G. et al. Structural characterisation of phosphate materials: new insights into the spatial proximities between phosphorus and quadrupolar nuclei using the *D*-HMQC MAS NMR technique. *Phys. Chem. Chem. Phys.* **13,** 16786–16794 (2011).

48. Haynes, W. M. in *Handbook of Chemistry and Physics* (ed. Ohio) 96 (CRC Press, 2015).

49. Brinkmann, A. & Kentgens, A. P. M. Proton-selective $^{17}O − ^1H$ distance measurements in fast magic-angle-spinning solid-state NMR spectroscopy for the determination of hydrogen bond lengths. *J. Am. Chem. Soc.* **128,** 14758–14759 (2006).

Author contributions

J.H., Y.J. and C.S. designed the study. Y.J. and A.B. prepared the samples. Z.W., O.L., J.T. and J.H. performed the NMR experiments and structural assignation. J.H. and J.-P.A. supervised the scientific work. J.H. and Z.W. contributed to writing the paper, and O.L., J.-P.A., A.B. and C.S. revised it.

Additional information

Supplementary Information accompanies this paper at http://www.nature.com/naturecommunications

Competing financial interests: The authors declare no competing financial interests.

Reprints and permission information is available online at http://npg.nature.com/reprintsandpermissions/

How to cite this article: Wang, Z. et al. Brønsted acid sites based on penta-coordinated aluminum species. *Nat. Commun.* **7,** 13820 doi: 10.1038/ncomms13820 (2016).

Publisher's note: Springer Nature remains neutral with regard to jurisdictional claims in published maps and institutional affiliations.